Received: 31 October 2023 | Revised: 8 July 2024 | Accepted: 9 July 2024

DOI: 10.1002/jemt.24659

RESEARCH ARTICLE

MICROSCOPY RESEARCH & TECHNIQUE WILEY

Amino acid surface modified bioglass: A candidate biomaterial for bone tissue engineering[1]

Yasin Özkabadayı[1] | Mustafa Türk[2] | Ali Kumandaş[3,4] | Siyami Karahan[1]

[1]Faculty of Veterinary Medicine, Department of Histology and Embryology, Kirikkale University, Kirikkale, Turkey

[2]Faculty of Engineering and Natural Sciences, Department of Bioengineering, Kirikkale University, Kirikkale, Turkey

[3]Faculty of Veterinary Medicine, Department of Surgery, Kirikkale University, Kirikkale, Turkey

[4]Faculty of Veterinary Medicine, Kyrgyz-Turkish Manas University, Bishkek, Kyrgyzstan

Correspondence
Yasin Özkabadayı, Faculty of Veterinary Medicine, Department of Histology and Embryology, Kırıkkale 71450, Turkey.
Email: y.ozkabadayi@kku.edu.tr

Review Editor: Alberto Diaspro

Abstract

Bioglasses are solid materials consisted of sodium oxide, calcium oxide, silicon dioxide and phosphorus in various proportions and have used in bone tissue engineering. There have been ongoing efforts to improve the surface properties of bioglasses to increase biocompatibility and performance. The aim of the present study is to modify the bioglass surface with an amino acid mixture consisting of arginine, aspartic acid, phenylalanine, cysteine, histidine and lysine, to characterize the surface, and to evaluate the performance and biocompatibility in vitro and in vivo. The untreated bioglass, bioglass kept in simulated body fluid (SBF), and modified bioglass were used in further evaluation. After confirmation of the surface modification with FT-IR analyses and SEM analyses, MC3T3-E1 preosteoblasts adhesion on the surface was also revealed by SEM. The modified bioglass had significantly higher ALP activity in colorimetric measurement, rate of calcium accumulations in Alizarin red s staining, lower rate of cell death in Annexin-V/PI staining to determine apoptosis and necrosis. Having higher cell viability rate in MTT test and absence of genotoxicity in micronucleus test (OECD 487), the modified bioglass was further confirmed for biocompatibility in vitro. The results of the rat tibial defect model revealed that the all bioglass treatments had a significantly better bone healing score compared to the untreated negative control. However, the modified bioglass exhibited significantly better bone healing efforts especially during the first and the second months compared to the other bioglass treatment treatments. As a result, the amino acid surface modification of bioglasses improves the surface biocompatibility and osteogenic performance that makes the amino acid modified bioglass a better candidate for bone tissue engineering.

[1] This article was produced from the doctoral thesis titled "Modified bioglass: in vitro and in vivo efficacy evaluation by means of hard tissue engineering".

Research Highlights

- Bioglass surface modification with amino acids contributes to bioglass-tissue interaction with an improved cell attachment.
- Modified bioglass increases in vitro Alp activity and calcium accumulation, and also positively affects cell behavior by supporting cell adaptation.
- Bioglass exerts osteogenic potential in vivo especially during early bone healing.

KEYWORDS
amino acid modification, biocompatibility, bioglass, bone tissue engineering

1 | INTRODUCTION

Bone tissue has a good regeneration capability by not forming scar tissue during the healing process (Marsell & Einhorn, 2011). Although anatomical reduction and stable fixation are necessary in fracture healing, many other factors including osteoblasts, osteoclasts, growth factors, hormones, age, nutrition, and chronic diseases can also affect the healing process (Keating et al., 2005). Even if the well-organized fracture healing process continues in a normal pathophysiological state, presence of other clinical conditions such as skeletal defects, avascular necrosis and osteoporosis can be highly influential on fracture healing (Raisz, 1999). In addition, open fractures (especially open tibia fractures) with soft tissue loss and periosteal detachment as a result of severe trauma, blast injuries, infection or tumor resections that require extensive debridement can also lead to critical bone loss (Keating et al., 2005). Fractures with extensive bone loss needs additional interventions to augment the healing process (Keating et al., 2005).

The bone tissue engineering strategies include the use of components such as cells, growth factors and scaffolds for repair and regeneration. Although biomaterial systems containing biological components are potentially valuable, difficulties in clinical practice and high cost are limiting factors for the use of these components. Therefore, bone tissue engineering applications mostly prefer the use of materials (Atala et al., 2012; Hunter & Sherman, 2017). Bioactive glasses are among the biomaterials used for bone regeneration. Bioactive glasses are hard and solid materials consisted of sodium oxide, calcium oxide, silicon dioxide and phosphorus in various proportions (Hench et al., 1971). A biologically active hydroxyapatite layer is formed where bioactive glasses come into contact with host tissue in the physiological environment (Cao & Hench, 1996). Substances such as silicon, sodium, calcium, and phosphate released during the degradation process also stimulate cells to synthesize new tissue (Cao & Hench, 1996). However, there are some current problems encountered in previous studies on bioglass, for example, insufficient interaction of the bioglass surface with the host tissue (Baino et al., 2018). Events such as cell adhesion, adhesion or activation of proteins, and the host immune response to the biomaterial occur at the biomaterial-tissue interface, and these biological events are determined by the physical and chemical properties of the biomaterial surface. Therefore, surface modification of biomaterials without changing their bulk (volume) properties seems to an acceptable approach with promising results not only for better attachment but also increased biocompatibility (Anderson, 2001; Anderson et al., 2008). Among the biomolecules used in surface modification of biomaterials are amino acids, which have isoelectric points depending on the functional groups and side chains in their structures (Agarwal & García, 2019; Lee et al., 2012; Uddin et al., 2010). Having such surface properties provide changes in the surface charge of amino acids. The electrostatic attraction between the amino acid and the biomaterial surface can be modulated by pH adjustment to attach acidic or basic amino acids on the biomaterial surface (Lee et al., 2013). The present study aimed to improve biocompatibility of bioglass by surface modification. For this aim, the bioglass surface was modified with a mixture of amino acids consisting of arginine, aspartic acid, phenylalanine, cysteine, histidine, and lysine. Then, the bioactivity and biocompatibility of the modified bioglass were evaluated by in vitro and in vivo experiments.

2 | MATERIALS AND METHODS

2.1 | Modified bioglass synthesis

The bioglass used in this study is the bioglass known as "45S5 Bioglass®" (Hench et al., 1971) and will be referred to as untreated bioglass in this study. The modification solution of bioglass was prepared by adding a mixture of amino acids to simulated body fluid (SBF). First, SBF was prepared (Kokubo and Takadama, 2006), then the amino acid mixture was added into the SBF. The final solution (100 ml) had the followings: L-lysine (50mg/100ml), L-histidine (50mg/100ml), arginine (100mg/100ml), aspartic acid (100mg/100ml), phenylalanine (100mg/100ml) and cysteine (100mg/100ml). The bioglass sample was placed in the mixture in a 250 ml conical glass container and kept in a shaking oven (KUHNER SHAKERX, Climo-Shaker ISF1-XC, and Switzerland) at 37 °C and 80 rpm for 25 days. Then, the fluid part was removed and the remaining part, modified bioglass, was dried overnight at 37 °C. For in vitro and in vivo tests, 3 different bioglass samples were used: untreated bioglass, modified bioglass, and bioglass kept in SBF.

2.2 | Modified bioglass characterization

2.2.1 | FT-IR spectrum

The FT-IR spectra of the bioglasses were measured using the VERTEX 70v FT-IR spectrometer (Bruker).

2.2.2 | Scanning electron microscopy imaging

The shape and topography of the bioglasses were examined using a scanning electron microscope (JEOL, JSM-5600). For SEM examination, the bioglass samples were dried, fixed on brass plates with an adhesive tape, coated using a gold sputter coating device (SBC-900-C sputtering coater), and examined.

2.3 | In vitro efficacy and biocompatibility tests

L929 fibroblast and Chineese Hamster Ovary CHO cell lines were obtained from the Sap Institute of the Turkish Ministry of Agriculture and MC3T3-E1 preosteoblasts was generosity of Prof. Halil Murat Aydin of Hacettepe University.

2.3.1 | Cell adhesion test

MC3T3-E1 mouse preosteoblast cell line was used in the cell adhesion test. The cells were cultured in Dulbecco's modified Eagle's medium (DMEM, Low Glocose, Biological Industries, Lot 2027500) containing 10% fetal bovine serum (Foetal Bovine Serum, Biological Industries, Lot 2004013) and 1% penicillin-streptomycin (Pen-Strep Solution, Biological Industries, Lot 1952187). To provide the basal environment to better facilitate interaction between the biomaterial and cells, the sterile bioglass materials were first placed in a 24-well plate and cell cultıure medium was added on to them before incubation for an hour at 37 °C in an environment condition with %5 CO_2. Upon withdrawing the culture meadia, cells were seeded on the biomaterial at a concentration of 5x104 cells/well and kept 4 hours to ensure cell adhesion, and then a ready-made culture medium until covering the top of the biomaterial. The cell seeded biometarials were kept for different time points: 3, 7 and 14 days, and cell adhesion along with cell morphology was evaluated with SEM. Prior to SEM analyses, the cell culture medium in the wells containing the cell seeded biomaterials were removed, and the well was washed twice with PBS before fixing the cells with 4% paraformaldehyde for 30 minutes. Following removal of paraformaldehyde in the wells and washing twice with PBS for 5 minutes each, the cell seeded biomaterials were dehydrated in an alcohol series: 30%, 50%, 70%, 80%, 96% and absolute alcohols. After a drying process, the surface of the cell-seeded biomaterials was coated with gold using the sputter coater device and examined with SEM.

2.3.2 | Alkaline phosphatase activity

ALP activity was measured by a colorimetric method, in which the SensoLyte pNPP (Catalog no: 72146) kit was used. For this purpose, 12.5x103 MC3T3-E1 preosteoblast cells per well were planted in 24-well plates, and ALP activity on MC3T3-E1 preosteoblast seeded bioglasses were measured on the 3rd, 7th and 14th days of cultivation in 3 replicates. At the end of the experiment periods, the absorption values of the cell extract, which was subjected to the procedures specified in the test kit protocol, were measured in an Elisa reader at a wavelength of 405 nm, and the ALP activity was calculated in ng/ml.

2.3.3 | Demonstration of calcium deposits with Alizarin Red S

Two different methods were used to evaluate calcium deposits: colorimetric method and Alizarin Red S staining. Colorimetric measurement was performed as stated by Quarto et al. (2015). For this purpose, 5x104 MC3T3-E1 preosteoblast cells per well were seeded in 24-well plates, calcium deposits on MC3T3-E1 preosteoblast seeded bioglasses were measured on the 3rd, 7th, and 14th days of cultivation in three replicates. Alizarin Red S amounts showing calcium accumulation were calculated in mM. Similarly, bioglasses of the 3rd, 7th, and 14th days of cultivation were stained with Alizarin red staining in which 2% Alizarin Red S (Kim et al., 2013) was adjusted to a pH of 4.1–4.3. The stained samples were then viewed under an inverted microscope (Leica DMI 6000B).

2.3.4 | Apoptosis-necrosis test

Annexin V-FLUOS Staining Kit (ROCHE) was used to evaluate the apoptosis-necrosis rates. Briefly, MC3T3-E1 cells were seeded on the bioglasses (5x104 MC3T3-E1 preosteoblast cells per well were seeded in 24-well plates) and kept for 3, 7 and 14 days. At the end of incubation, the medium was discarded, and the prepared Annexin-V and propidium iodide (PI) dye solution was added on the cells. Upon keeping the cell seeded biomatarials for 15 minutes at room temperature in the dark, cells on the biomatarials were examined under an inverted microscope (Leica DMI 6000B) using the FITC fluorescent filter. The cell membrane of apoptotic cells illuminate green floure-censce (FITC) while the nucleous of the necrotic cells illuminate red flourence (PI). The healty cells do not illuminate neither of them.

2.3.5 | In vitro cytotoxicity testing

Cytotoxicity of modified bioglass were evaluated by a direct method, MTT (3,[4,5-dimethylthiazol-2-yl]-2,5-diphenyltetrazolium bromide) test, a cited method in ISO 10993–5 standard for in vitro biocompatibility. Briefly, L-929 fibroblasts and MC3T3-E1 preosteoblast cells were seeded at a densitiy of 1.0x 104 cells/well in a 96-well plate,

then the modified bioglass was extracted in cell medium and the obtained extract (0.2g/ml) was exposed to cells. After 24 h of incubations, MTT was added to cell containing wells and kept for 2 h. After removal of MTT and addition of isopropyl alcohol, the absorbance values were measured at 570 nm wavelength in an Elisa Reader (SPECTROstar Nano- S/N 601–1841). The cell viability was calculated using the following formula: % cell viability = (absorbance value of test sample/negative control absorbance value) × 100. If the cell viability is above 70%, the samples passes the test and meets the requirement for in vitro biocompatibility criteria.

2.3.6 | In vitro micronucleus test

In vitro micronucleus test was conducted in accordance with ISO 10993-3 and OECD 487 standards to determine the genotoxicity potential of the test product. Briefly, the CHO cell line specified in the standard was exposed to the extracts obtained from the bioglass samples. Firstly, cells at a density of 15x103 were seeded into 48-well plates. The cells were incubated for 24 hours (37°C, 5% CO2). At the end of the incubation period, the culture media in the wells were discarded and three different concentrations of the extract (1:1, 1:2, and 1:4) were added to the wells and kept either for 3 hours or 24 hours. In the short period test (3 hours), the test was conducted either in the presence of absence of S9 (2%), which was added along with test extract if used. After incubation for 3 hours, the cell culture medium was removed and a fresh medium containing cytochalasin B (3μg/ml) for was added into the wells. In the long period test (24 hours), the test extract and the cytochalasin B (3μg/ml) containing fresh extract were added into the wells. Mitomycin C and cell culture medium was used as positive and negative controls, respectively. At the end of the experiment, the media in the well was discarded and 200 μl of 75 mM KCl was added to the wells. After 5 min of incubation, KCl was removed and a mixture of methanol and glacial acetic acid (3:1) was added into wells to fix the cells. After that, the fixatative mixture was replaced with PI dye, which stains cell nuclei. The mononucleated, binuclated, and multinucleated cells were counted under an inverted florescence microscope. The micronucleus rates, Cytokinesis Block Proliferation Index (CBPI) and cytostasis were calculated as specified in the standard.

2.4 | In vivo tests

The in vivo experiments were carried out upon approval by the Kırıkkale University Institutional Ethics Committee for Animal Experiment (Protocol No: 2021/09–34). All animal experiments were carried out at the Kırıkkale University Hüseyin Aytemiz Laboratory Animal Research Facility.

2.4.1 | Implantation and extremity performance test

The protocols specified in ISO 10993-2-6-12 standards for interosseous implantation were used to assess the local effect after implantation. A total of 84 wistar albino male rats weighing 222.26 ± 50.04 g were used. Under general anesthesia, unicortical critical size defects of 4 mm wide and 4 mm long were created in the antero-medial cortex of the proximal tibia. Animals were randomly assigned to one of the following four groups, each having seven rats: modified bioglass, untreated bioglass, bioglass kept in SBF and negative control. Following implantation, animals were euthanatized at the end of the 4th, 8th, and 12th weeks. The defect sites were removed and placed in 10% formalin for 72 h, decalcified in % 10 formic acid solution, and embedded in paraffin following the routine dehydration process. Then, 5 μm thick sections were cut from paraffin blocks and stained with Masson's triple stain and hematoxylin–eosin. The sections were examined under a light microscope (Nicon Eclipse 50i) and the defect sites were analyzed using two different scoring systems: the Emery scoring system for tissue integration and performance (Emery et al., 1994) and the semi quantitative histopathological scoring cited in ISO 10993–6 Tables 1 and Table 2 (Annex 5) (ISO 10993-6, 2016) for assessment of local irritant effect following implantation.

TABLE 1 Histopathological evaluation of the bone defect according to the Emery scoring system.

Score	Evaluation criteria
0	Defect area is empty
1	There is only fibrous connective tissue in the defect area
2	There is more fibrous connective tissue than fibrous cartilage
3	There is more fibrous cartilage than fibrous connective tissue
4	There is only fibrous cartilage
5	There is more fibrous cartilage than bone
6	There is more bone than fibrous cartilage
7	It is just full of bone

TABLE 2 ISO 10993–6 Table 1 (Annex 5)—Semi quantitative histopathological scoring.

Animal number	Sample
A1. Inflammation	
Polymorphonuclear cell	Score (0–4)
Lympocytes	Score (0–4)
Plasma cells	Score (0–4)
Macrophages	Score (0–4)
Giant cells	Score (0–4)
Necrosis	Score (0–4)
Subtotal (×2)	
A2. Neovascularization	Score (0–4)
Fibrosis	Score (0–4)
Fatty infiltrate	Score (0–4)
Subtotal	
Total	A1 + A2
Average	
Score	Test − Control

Note: Irritation scores: None (0.0–2.9); mild (3.0–8.9); medium (9.0–15.0); Severe (>15.0).

2.5 | Statistical evaluation

A SPSS statistical program was used to evaluate in vitro and in vivo test results. Data obtained from the colorimetric tests of ALP activity and Alizarin Red S and calcium deposits were compared among groups using ANOVA test. Data obtained from the In vitro micronucleus test were statistically evaluated with the Fisher's exact test. For data obtained from the Emery scoring of the bone defect, the Kruskal-Wallis test was used to determine presence of a significant difference, and the Mann–Whitney test was used for multiple comparisons.

3 | RESULTS

3.1 | FT-IR spectrum

The FT-IR spectrum of the regular bioglass was in 97.09% correlation with the reference sample (45S5 Bioglass powder, Mo-Sci Corporation) since the absorption peaks were very similar (Figure 1).

The FT-IR spectra obtained from the untreated bioglass (Figure 2) exhibited peaks among which the peak numbers of 1019 and 919 (cm^{-1}) indicate the Si—O—Si bending stress and the Si—O—Si asymmetric stress, respectively. In addition, the peaks of Si bonds confirm the presence of the glassy structure, an important feature of bioglass. On the other hand, the modified bioglass has absorption peaks of (Figure 2), among which the peak numbers of 1059, 952, 598, and 451 are strong bands vibration peaks showing bonds formed between P and O that confirms the existence of the hydroxyapatite layer formed on the surface. The bioglass kept in SBF, another treatment, has the absorption peaks (Figure 2), among which the peak numbers of 1064, 942, 597, and 454 (cm^{-1}) are the bonds formed between P and O, showing the presence of the hydroxyapatite layer. Unlike the untreated bioglass and bioglass kept in SBF, the modified bioglass has an absorption peak number of 1554 cm^{-1} (Figure 2). This peak is due to the N—H bending vibration in amino groups. If so, this peak confirms the presence of amino acid coating on the modified bioglass surface.

3.2 | SEM imaging

SEM images of the untreated bioglass revealed that the surface has amorphous structures, and there are no hydroxyapatite crystals on the surface (Figure 3a). On the other hand, the SEM images of the modified bioglass revealed the presence of clearly outlined porous structures (Figure 3c), surface accumulation of a certain type of a substance in a mottled appearance throughout the surface in a similar manner, likely indicating amino acid accumulation (Figure 3c), and the hydroxyapatite crystals (Figure 3d). The bioglass kept in SBF exhibited hydroxyapatite crystals on surface (Figure 3b). All SEM images are compatible with FT-IR measurements.

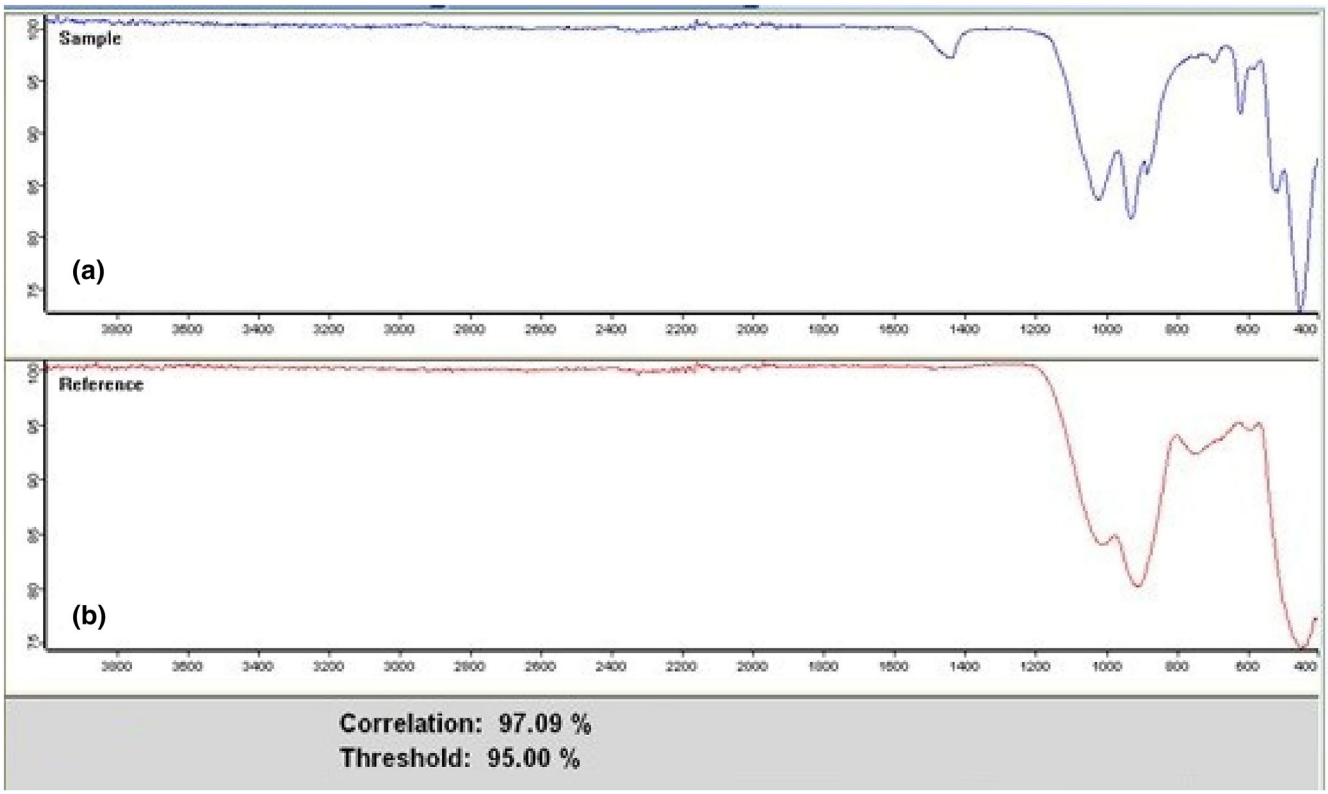

FIGURE 1 FT-IR comparison of the untreated bioglass (a) with reference sample (b).

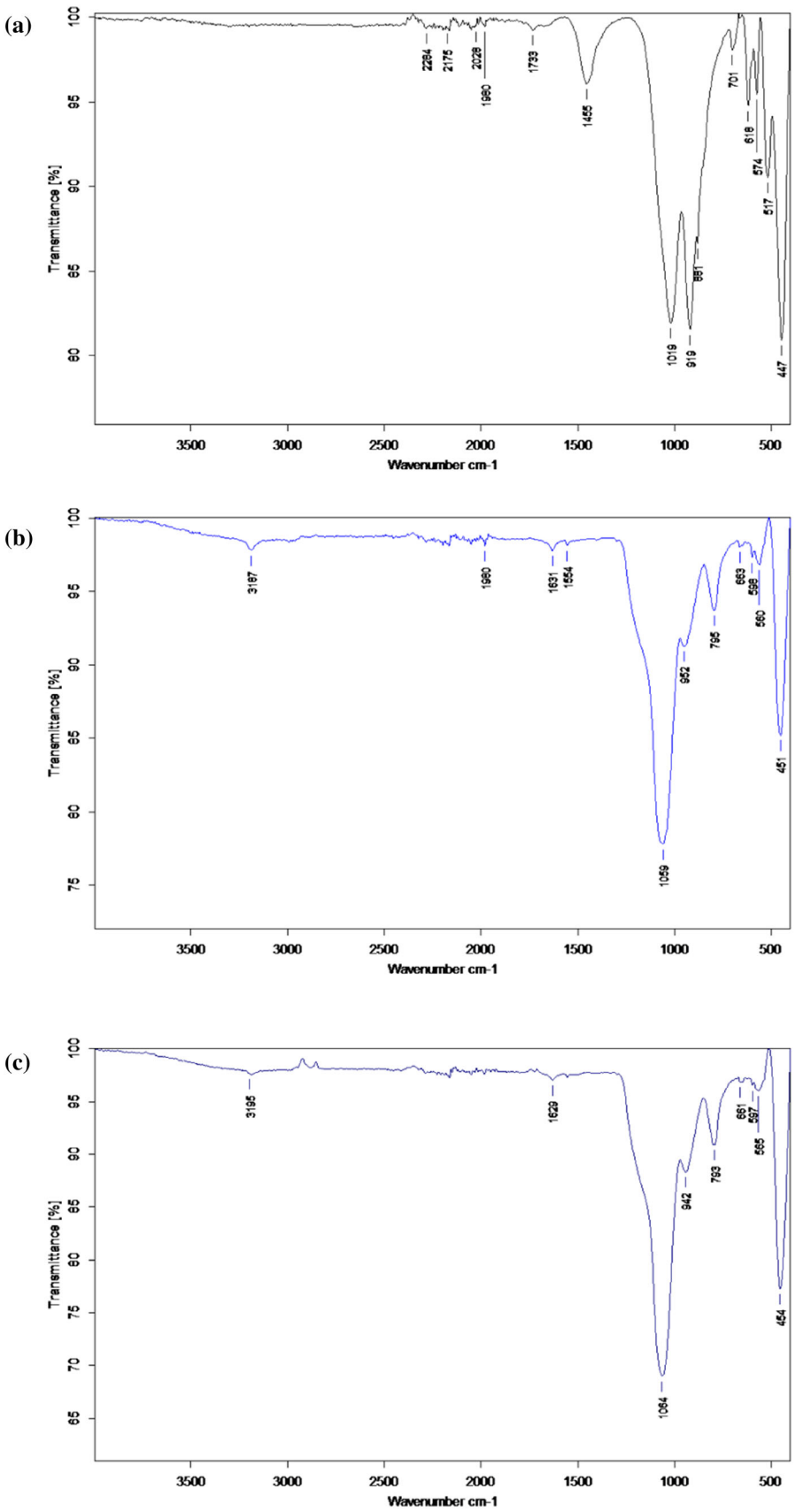

FIGURE 2 FT-IR spectrums of the untreated bioglass (a), modified bioglass (b), and bioglass kept in SBF (c).

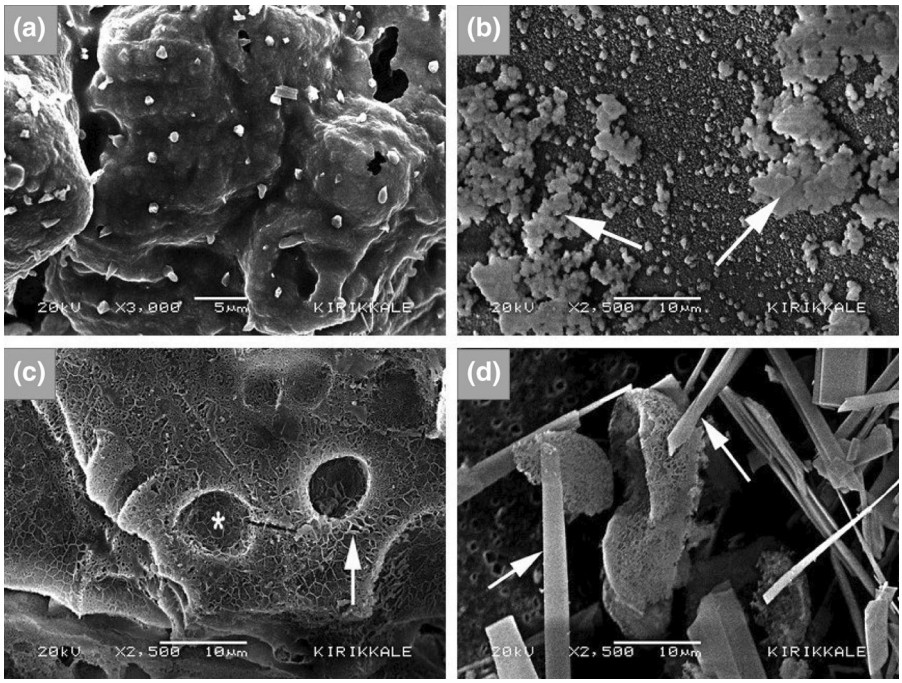

FIGURE 3 SEM images of the untreated bioglass (a), bioglass kept in SBF (b) and modified bioglass (c-d). In photomicrographs, a) the untreated bioglass has an amourphous surface structures, b) bioglass kept in SBF showed surface accumulations of hydroxyapatite (arrows), c) the modified bioglass has clearly marked pours (star), surface accumulation of a substance throughout the surface (arrow), and d) the modified bioglass has also hydroxyapatite crystals (arrows). SBF=simulated body fluid.

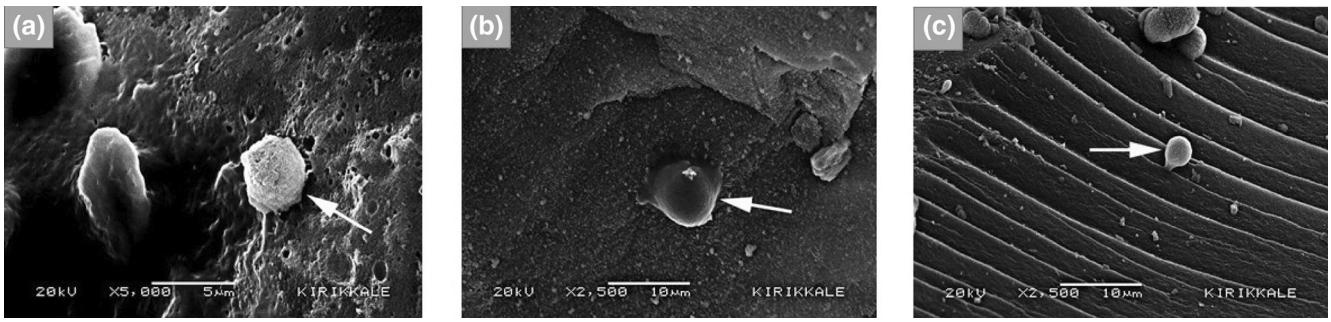

FIGURE 4 SEM images of MC3T3-E1 cells seeded on bioglass. a) Cell with cell extensions on the surface (arrow) are the most frequently seen on the modified bioglass surface, b) cell adhering to the surface also appears in the bioglass kept in SBF, c). Cell attachment on the surface is weaker and cells frequently appear in round morphology in the untreated bioglass. SBF=simulated body fluid.

3.3 | Results of in vitro efficacy and biocompatibility tests

3.3.1 | Cell adhesion

In SEM examination of the 3rd-day samples, cells seeded on the modified bioglass exhibited a spheroid morphology with cell extensions attaching to the material surface (Figure 4a). Cells seeded on the bioglass kept in SBF also expressed adherence to the surface of the material (Figure 4b). Unlike on the modified bioglass and bioglass kept in SBF, cells seeded on the untreated bioglass had a limited number attached cells. Cells were frequently spheroid in shape with no apparent signs of attachment (Figure 4c).

In SEM examination of the 7th-day samples, cells seeded on the modified bioglass, the attached cells on the surface expressed a squamous morphology with cell extensions (Figure 5a,b). A large number of attached MC3T3-E1 cells were also present in spheroid morphology (Figure 5c). The spheroid cells were frequently observed in groups. Cells seed on the bioglass kept only in SBF were seen in spheroid morphology and frequently colonized (Figure 5d). Cells seeded on the untreated bioglass, a small number of attached cells with spheroid morphology were observed (Figure 5e). Cells in squamous morphology with cell extensions were observed neither on the surface of the bioglass kept in SBF nor on the untreated bioglass.

In SEM examination of the 14th-day samples, cells seeded on the modified bioglass, a large number of cells with spheroid morphology (Figure 6a) and cells with squamous cell morphology and extensions in different areas were observed. Cells seed on the bioglass kept only in SBF were seen in spheroid morphology attaching to the surface (Figure 6b). Cells seeded on the untreated bioglass, a small number of cells with spheroid morphology are present, attaching to the surface (Figure 6d).

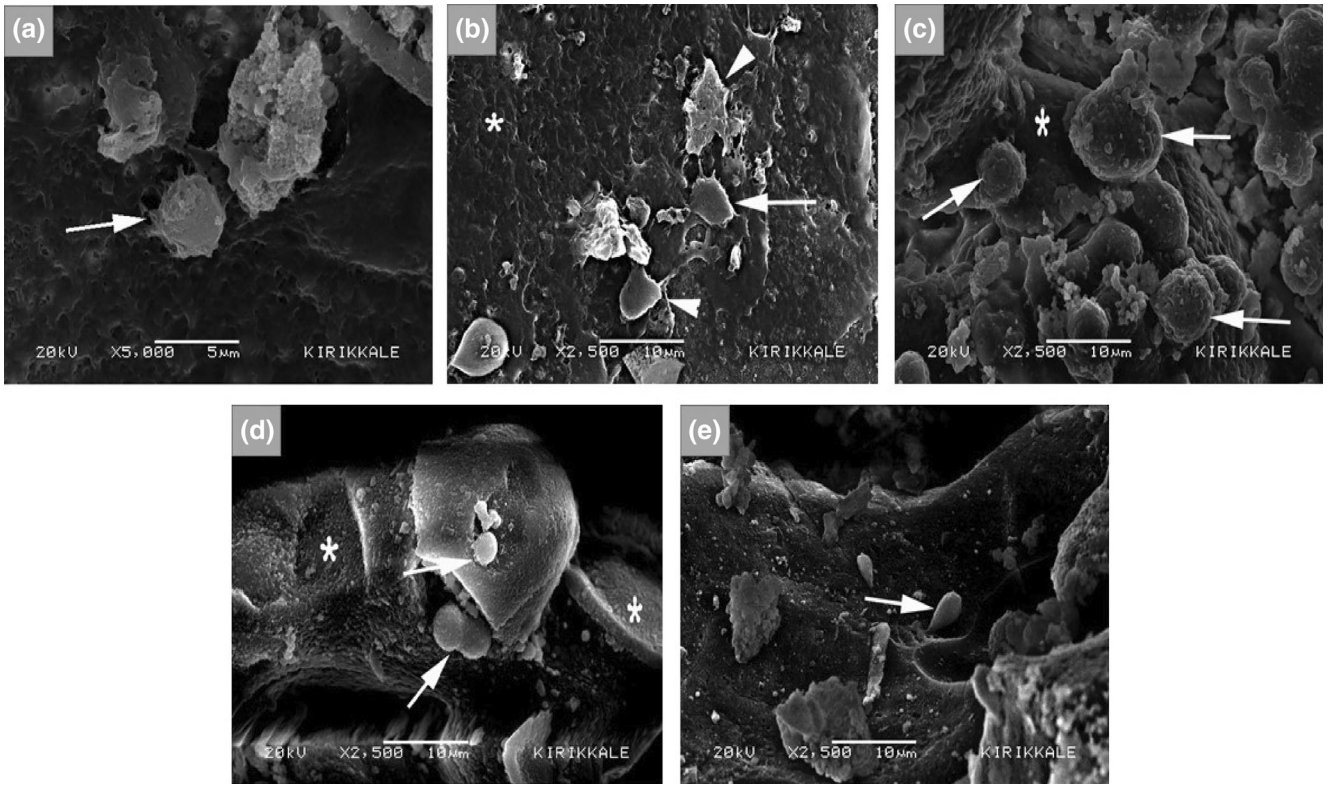

FIGURE 5 SEM images of MC3T3-E1 cells seeded on modified bioglass (a,b, and c), bioglass kept in SBF (d) and untreated bioglass (e) at day 7. a) Cell (arrows) appears as attaching to the surface with cell extensions adhering to the modified bioglass surface, b) Cells appeared in squamous morphology with (arrow) and cell extensions (arrows and arrow heads) adhering to the modified bioglass surface (star), c) Numerous cells in spheroid morphology (arrows) are also seen in modified bioglass, d) In bioglass kept in SBF, a small number of cells in spheroid morphology appearred as adhering to the surface (*), and e) cells in spheroid morphology (arrow) also seen in untreated bioglass surface. However, the number of cells on the surface was the least. SBF=simulated body fluid.

FIGURE 6 SEM images of MC3T3-E1 cells seeded on modified bioglass (a, b), bioglass kept in SBF (c), and untreated bioglass (d) at day 14. a) Cells (arrows) appears as proliferating and attaching to the surface numerous cells with spheroid morphology adhering to the modified bioglass surface, b) Cells appeared in squamous morphology with and cell extensions (arrow and arrow head) adhering to the modified bioglass surface, c) in bioglass kept in SBF, a less number of cells (arrows) in spheroid morphology appearred as adhering to the surface (*), d) cells in spheroid morphology (arrows) also seen in untreated bioglass surface(*). However, the number of cells on the surface was the least. SBF=simulated body fluid.

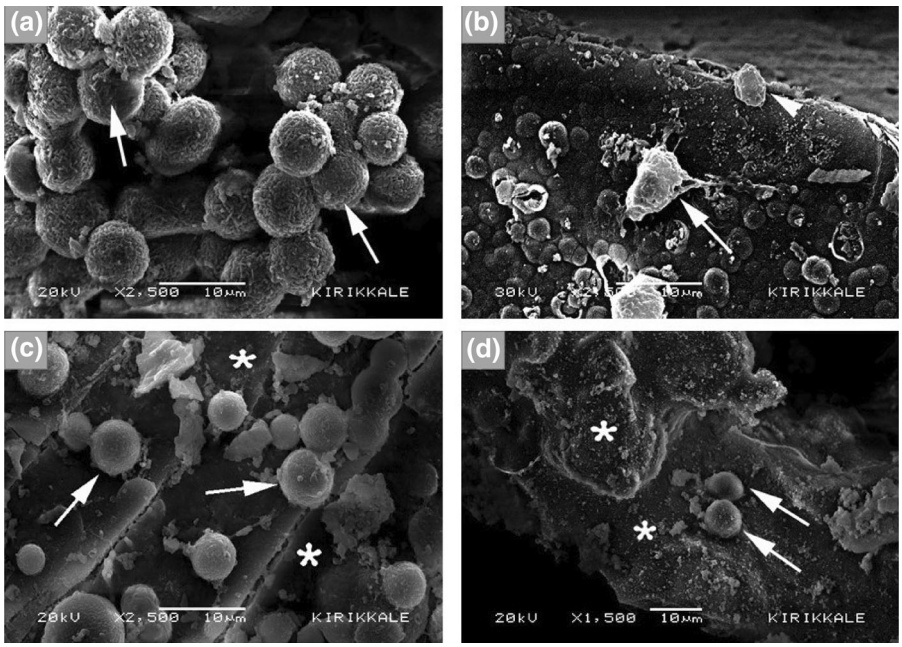

3.3.2 | In vitro ALP activity

Table 3 present the ALP activity data in ng/mL. In the third and seventh day samples, the ALP activity of the modified bioglass group was significantly higher compared to those of the untreated bioglass and negative control, but not the bioglass kept in SBF although it tends to be significant ($p = .055$) (Table 3). In the 14th day samples, the modified bioglass had the highest amount of ALP activity compared to all.

3.3.3 | Alizarin red S staining

Microscopic examination of alizarin red S staining

The inverted microscope images of the 3rd day of the cells seeded in modified bioglass revealed the areas of calcium deposition are observed to a large extent in the culture medium (Figure 7). Cells inoculated on bioglass kept in SBF, had less calcium deposited areas compared to the modified bioglass (Figure 7). Cells seeded on the

TABLE 3 Group and time-dependent variation of in vitro ALP activity (ng/mL).

	Modified bioglass	Bioglass kept in SBF	Untreated bioglass	Negative
3rd day	2.053 ± 0.46[a]	1.656 ± 0.502[a]	0.920 ± 0.163[b]	0.640 ± 0.20[c]
7th day	2.10 ± 0.503[a]	1.711 ± 0.312[a]	1.221 ± 0.298[b]	0.957 ± 0.14[c]
14th day	2.893 ± 0.514[a]	1.942 ± 0.718[b]	1.542 ± 0.28[b.c]	1.33 ± 0.38[c]

Note: Data are given as mean ± std. Different letters in the same row indicate significant differences.

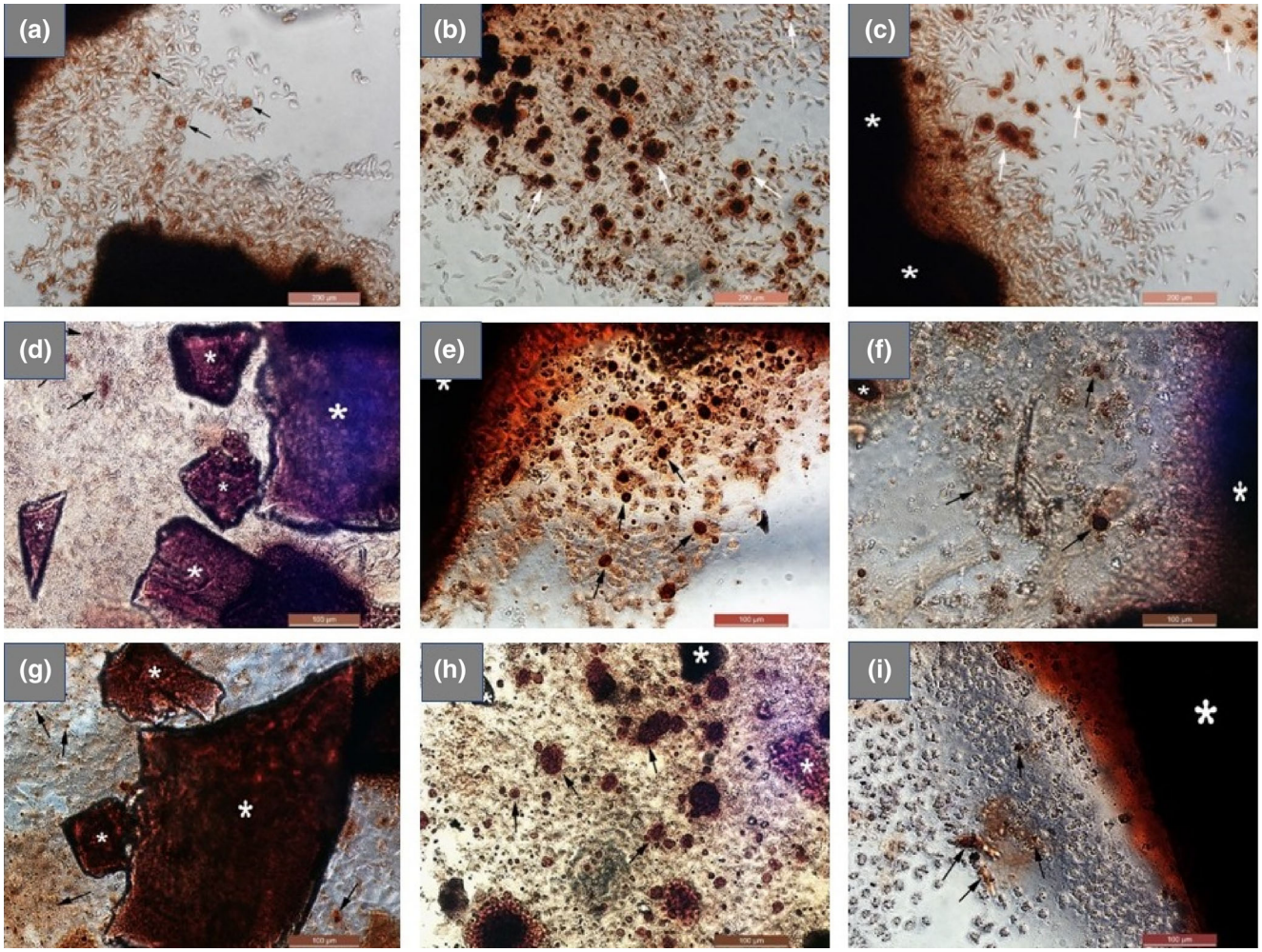

FIGURE 7 Alizarin Red S staining images of MC3T3-E1 cells seeded on biomaterials. b, e, h) compared to other bioglasses, modified bioglass had the most intense alizarin red staining intensity and largest stained areas at the 3rd day, 7th day and 14th day, respectively. c, f, i) the bioglass kept in SBF had stained areas but less intense and smaller areas compared to the modified bioglass. a, d, g) Compared to the others, the untreated bioglass had the least intense staining. In all photographs, arrows indicate areas stained with Alizarin red and stars indicate biomaterial. Alizarin Red staining, SBF= simulated body fluid.

TABLE 4 Group and time-dependent variation of in vitro Alizarin Red S concentration (mM).

	Modified bioglass	Bioglass kept in SBF	Untreated bioglass	Negative
3rd day	0.09 ± 0.015[a]	0.06 ± 0.012[a.b]	0.03 ± 0.005[b.c]	0.02 ± 0.002[c]
7th day	0.18 ± 0.011[a]	0.14 ± 0.006[b]	0.13 ± 0.009[c]	0.05 ± 0.004[d]
14th day	0.36 ± 0.012[a]	0.30 ± 0.006[b]	0.25 ± 0.010[c]	0.17 ± 0.005[d]

Note: Data are given as mean ± std. Different letters in the row indicate significant differences.

TABLE 5 The cell viability apoptotic and necrotic rates of MC3T3-E1 cells cultivated on the modified bioglass determined on the 3rd, 7th and 14th days of cell culture.

3rd day	Viability %	Apoptosis %	Necrosis %
Modified Bioglass	98.23 ± 0.05[a]	1.29 ± 0.15[a]	0.46 ± 0.10[a]
Bioglass Kept in SBF	94.54 ± 0.18[b]	4.54 ± 0.96[b]	0.90 ± 0.85[b]
Untreated Bioglass	90.26 ± 1.03[c]	7.69 ± 2.43[c]	2.05 ± 0.97[c]
7th Day			
Modified Bioglass	96.43 ± 0.60[a]	2.77 ± 0.55[a]	0.78 ± 0.04[a]
Bioglass Kept in SBF	94.50 ± 1.21[b]	5.03 ± 0.74[b]	0.45 ± 0.15[a]
Untreated Bioglass	93.33 ± 5.43[b]	4 ± 1.34[c]	2.66 ± 0.95[b]
14th Day			
Modified Bioglass	95.29 ± 0.09[a]	3.93 ± 0.46[a]	0.77 ± 0.37[a]
Bioglass Kept in SBF	93.54 ± 3.56[b]	4.83 ± 1.12 [a]	1.61 ± 0.18[b]
Untreated Bioglass	81.84 ± 3.65[c]	13.03 ± 1.21[b]	5.12 ± 4.87[c]

Note: Data are presented as in mean ± std. The mean difference is significant at the 0.01 level. Data with different superscripted letters in the same column of the same day are significantly different.

untreated bioglass, had the least calcium accumulated areas (Figure 7). On the 7th and 14th days of cultivation, the calcium deposits with better staining spreaded much larger areas in modified bioglass (Figure 7). The results are reflected in spectrophotometric measurements for which a statistical analysis was conducted (see below).

Colorimetric measurement of alizarin red S staining

Table 4 presents the Alizarin Red S concentrations given at mM levels. In the spectrophotometric measurements of the 3rd day of cultivation, the Alizarin Red concentration was significantly higher compared to those of the negative control (p: .035) and untreated bioglass samples (p: .039), but that of the bioglass kept in SBF (p: .069). The modified bioglass had higher amount of Alizarin Red concentrations compared to the others at the 7th and 14th days of cultivation (p: .007, p: .0003, respectively). Furthermore, the Alizarin Red S concentration was the lowest in the samples of the untreated bioglass out of negative control (p: .0001).

3.3.4 | In vitro apoptosis-necrosis test

In Annexin V test, the viability rates in MC3T3-E1 preosteoblasts were significantly different among the cells exposed to the different bioglasses at the 3rd, 7th and 14th days of cultivation ($p < .01$). The cell viability was the highest in the cells cultivated on the modified bioglass at all measurement days while the cells incubated with the untreated bioglass had the lowest cell viability rate. (Table 5). The Annexin V test further revealed apoptotic and necrotic rates in MC3T3-E1 preosteoblasts. The apoptotic rates were significantly higher compared to the necrotic rates for all treatments at all time points ($p < .01$).

TABLE 6 Cell viability rates (%) in MTT test following incubations of cells with various concentrations of the modified bioglass extract.

Concentration	L-929 Viability (% mean ± SD)	MC3T3-E1 Viability (% mean ± SD)
0.2 g/mL (1:1)	84.64 ± 11.63	86.94 ± 11.95
Positive Control	37.00 ± 4.05	41.13 ± 7.69

Note: Cell viability lower than 70% is considered as having cytotoxicity potential.

3.3.5 | In vitro cytotoxicity test

The results of the MTT test indicated that the highest concentration of the modified bioglass extract (0.2 g/mL) exposed to L-929 fibroblasts and MC3T3-E1 osteoblasts resulted in a cell viability rates of 84.64% ± 11.63% and 86.94 ± 11.95%, respectively (Table 6).

3.3.6 | In vitro micronucleus test

The micronucleus rate in CHO cells exposed to extract of the positive control was statistically higher compared to those of the modified bioglass and negative control (p: .00028) while there was no significantly

difference between the modified bioglass and negative control (Table 7). Therefore, it was concluded that the modified bioglass did not have a potential for genotoxicity.

3.4 | In vivo tests

3.4.1 | Bone defect and intramedullary implantation study

No incidence of animal death occurred and all animals completed the planned clinical period of study without any adverse effects in terms of general health status. The defect sites of the proximal tibia were evaluated histopathologically using the Emery scoring system for tissue integration and performance on the samples collected at the end of first, second, and third months of the surgery and treatment Table 8.

Table 8 and Figure 8 present the results of histopathological examination of the defect sites. Compared to the untreated bioglass and the bioglass kept in SBF, the modified bioglass had the defect site filled significantly with trabecular bone almost completely at the end of the first month ($p < .01$). In addition, there was trabecular bone formation in the medullary cavity. In the negative control group with no bioglass treatment, the defect area was completely filled with fibrous tissue. At end of the second month, the bone formation in the defect site treated with the modified bioglass had improved bone healing with the formation of the secondary bone lamellae. A similar observations were made in the defect sites treated with the bioglass kept in SBF; however, the cortical bone around the defect site was thinner. Although it was significantly better in the untreated bioglass compared to the negative control ($p < .01$), the defect sites and the medullary cavity exhibited bone formation activity in both groups. At the end of the 3rd month, the defect sites were closed with trabecular bone in all groups; however, the secondary bone lamellae were higher in the modified bioglass group with the cortical bone of sufficient thickness.

The defect site was also evaluated for local irriation following the intramedullary implantation of bioglasses conducted according to the 10,993–6 standard. No irritant effects were observed at any time points in any groups. The local response to the bioglasses was characterized by very low macrophage response, limited neovascularization and fat infiltration. Fibrosis was relatively lower in the modified bioglasses at the end of the first month compared to the untreated bioglasses and the bioglass kept in SBF.

TABLE 7 Statistical comparison of the calculated micronucleus ratios (%) in the in vitro micronucleus test.

	Micronucleus rates (%) 3 h with S9	Micronucleus rates (%) 3 h without S9	Micronucleus rates (%) 24 h without S9
MB 1:1	1.36[a]	1.4[a]	1.56[a]
MB 1:2	1.19[a]	1.17[a]	1.17[a]
MB 1:4	1.12[a]	1.2[a]	1.18[a]
Negative control	0.97[a]	0.95[a]	0.99[a]
Positive control	13.6[b]	13[b]	14.62[b]

Note: Different letters in the same column indicate statistical difference.

4 | DISCUSSION

The surface properties of the biomaterials generally determine their biocompatibility and degree of tissue integration, thus researches focused on modification of the surface properties of the biomaterials (Anderson, 2001; Anderson et al., 2008; Variola et al., 2009). Hydroxyapatite and additional amino acid modification of the bioglass were among the aim of the present study. In FT-IR examination, the various absorption peaks observed in the modified bioglass and the bioglass kept in SBF confirmed the presence of hydroxyapatite formed on the surface of the bioglass, compatible with the literature data (Adawy et al., 2009; Bayraktar & Tas, 1999; Kundu et al., 2010; Mollazadeh et al., 2007; Tas, 2000). Furthermore, the absorption peak at the wavelength of 1554 cm^{-1}, belonging to the N—H bending vibration, was only seen in the modified bioglass (Silva et al., 2005; Zhang et al., 2007). The FT-IR peaks confirmed the presence of hydroxyapatite and additional amino acid modification of the bioglass surface. In addition, SEM studies revealed images complementary to the FT-IR outputs. The untreated bioglass samples had an amorphous structure without presence of any other surface structure. The SEM images of the untreated bioglass are similar to those observed in the previous studies (Ravarian et al., 2010; Saboori et al., 2009). The SEM images of the bioglass samples kept in SBF exhibited a rougher surface appearance, and the surface had crystalline structures. This image is similar to those in previously reported studies on the hydroxyapatite presence on the bioglass surface kept in SBF (Kasuga et al., 2001; Kim et al., 2003; Ohtsuki et al., 1992). In the modified bioglass

TABLE 8 Scores and statistical comparison of the groups evaluated according to the Emery scoring system of tissue integration and performance.

	Modified bioglass	Bioglass kept in SBF	Untreated bioglass	Negative
1st Month	3 (2–5)[a]	2 (1–3)[b]	2 (1–2)[b]	1 (0–2)[b]
2nd Month	6 (5–6)[a]	5 (4–6)[a]	4 (3–5)[b]	3 (1–4)[c]
3rd Month	6 (5–7)[a]	5 (4–6)[b]	5 (3–6)[b]	4 (3–5)[b]

Note: Data are given as median (minimum–maximum). Different letters on the same row indicate statistical difference.

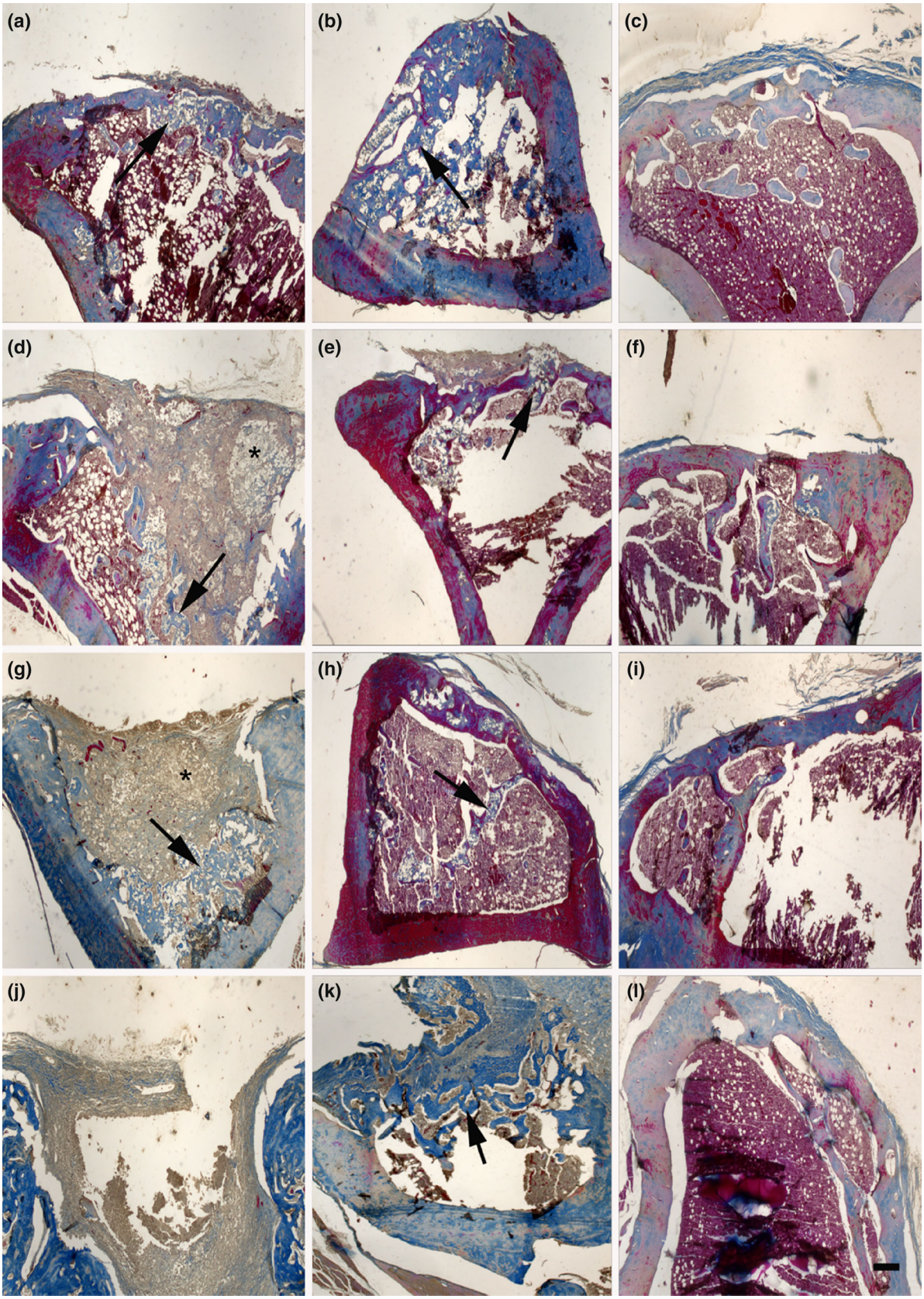

FIGURE 8 Legend on next page.

samples, in addition to crystalline structures of the hydroxyapatite layer there were clearly outlined porous structures and surface accumulation of a certain type of a substance in mottled appearance throughout the surface in a similar manner, likely indicating amino acid deposition on the surface. Thus, the FT-IR study to characterize the materials confirmed that hydroxyapatite and amino acid deposition of the surface.

Tissue integration of biomaterials is among the important parameters to evaluate biomaterials to be used in tissue engineering. In vitro cell attachment studies may give a clue for determination tissue integration properties of the biomaterials (Rahmany & Van Dyke, 2013). In the present study, MC3T3-E1 osteoblasts were incubated on the bioglasses and examined by SEM analyses. All types of bioglasses exhibited cell adhesions on the surface to various degrees on the samples of the 3rd day. However, especially on the samples of the 7th and 14th days of cultivation, the modified bioglass group exhibited a better cell adhesion capacity with a higher number of cells attached with spheroid and flat morphologies and distinct cytoplasmic extensions. Thus, the modified bioglass seems to have an improved cell adhesion property for MC3T3-E1 osteoblasts. The improved cell adhesion property most likely due to presence of functional groups such as NH_2 and COOH on the surface of the modified bioglass. Keselowsky et al. (2003) concluded that amino acid coated biomaterials increased the cell attachment capacity of materials due to presence of such functional groups. Squamous cell morphology on the surface has been reported to be as an indicator of osteogenic differentiation in vitro (Ventre et al., 2012). In addition, the prominent cell extensions in the squamous cells are also evidence of the cell adaptation of preosteoblast cells (MC3T3-E1) to the surface. Such SEM images indicate that MC3T3-E1 osteoblasts are well spread and tightly attached on the surface (Clupper et al., 2003).

Among early markers of the osteoblastic differentiation is ALP activity (Boanini et al., 2006). The differentiation process of preosteoblast cells (MC3T3-E1) includes proliferation, extracellular matrix maturation and mineralization stages (Beck Jr, 2003). In another word, osteoblast proliferation and differentiation precede bone mineralization (Beresford et al., 1993; Ramaswamy et al., 2008). It has been reported that some ions such as Ca, Sr released from bioglasses increase the metabolic activity of osteoblasts, ALP activity, osteogenic gene expression and matrix mineralization (Silver et al., 2001; Valerio et al., 2004). Addition of amino acids such as aspartic acid, arginine, and lysine to the medium increases osteoblast differentiation and extracellular mineralization (Rautaray et al., 2005; Sarig, 2004; Torricelli et al., 2002). In support to the previous studies, the results of the present study indicated that samples of the modified bioglass had a higher ALP activity compared to the untreated bioglass and bioglass kept in SBF. Furthermore, the results of histological staining and colorimetric measurement of Alizarin Red concluded that degree of mineralization is significantly higher in samples of the modified bioglass.

Osteoblast survival and adaption to biomaterials is critically important in bone tissue engineering (Mitra et al., 2013). The present study evaluated MC3T3-E1 cell viability, for which cells were inoculated and incubated with the bioglasses of different treatments for 3, 7, and 14 days. In addition, apoptotic and necrotic rates following incubation with the bioglasses were determined through Annexin V staining method. At all-time points, MC3T3-E1 cells incubated with the modified bioglass had lower rates of cytotoxicity and consequently lower apoptotic and necrotic rates. However, the differences were statistically significant among groups. Bioglasses of different treatments used in the present study seem to provide a suitable environment for preosteoblasts and to support their proliferation. However, although insignificant, the higher cell viability rate and the lower apoptotic and necrotic rates in MC3T3-E1 cells incubated with the modified bioglass can be considered as the best option to support osteoblast proliferation as a consequence of surface modification with amino acids (Boanini et al., 2006; Fini et al., 2001; Torricelli et al., 2001). The amino acids may have provided additional cytoprotective effect through participating in glutathione synthesis (Beutler, 1989). Apoptosis and necrosis are two different types of cell death (McConkey, 1998). Apoptosis is defined as a highly regulated natural biological process of programmed cell death in which the cell collapses and destroys itself (Kerr et al., 1972). By way of apoptosis, the organism eliminates the unwanted and aged cells to sustain the normal physiological functions and even to adapt to the environment in tissues of the developing organism and even in those of the adult. On the other hand, cell necrosis is defined as a cell injury in the presence of a harmful stimulus such as chemicals, pathogens, and mechanical disturbance. (Elmore, 2007; Lopez & Tait, 2015). The results of the Annexin V-PI analysis in the present study indicated that exposure to the bioglasses of all kinds caused very limited cell cytotoxicity, and the cell death mainly occurs through apoptosis, not necrosis. Thus, this finding further supports the biocompatibility properties of bioglasses as the extractables and leachables released from the bioglasses cause limited harmful effect on cells and tissues.

In general, bioglasses have a good in vitro biocompatibility (Comesaña et al., 2011; Gough et al., 2004). Our study indicated that the amino acid modified bioglass has an improved cell survival rate and attachment properties. The cytotoxicity test of the modified bioglass

FIGURE 8 Photographs of the bone defects treated with different bioglasses at the end of the first, second, and third months. a, b and c) The modified bioglass application resulted in a better bone formation (arrows) at al time points compared to the other teratments. d, e, and f) In the bioglass kept in SBF, the bioglass remnant are visible (stars) with a limited amount of bone formation /arrow) at the ent of the 1st month, which improved at the 2nd and 3rd month. g, h, and i) the untreated bioglass resulted in morphological changes similar to the bioglass kept in SBF. J, k, an l) The untreated control had no bone formation at the end of the 1st month; however, bone formation (arrow) seen at the end of the 2nd and 3rd months. Masson's trichrome staing. Bar= 400μm, SBF= simulated body fluid.

resulted in a very high cell viability in L929 fibroblasts and MC3T3-E1 preosteoblasts. Biomaterials especially those used for long terms may induce genotoxicity as a consequence of exposure and interaction of leached substances with cellular nuclear materials (Mohanan & Rathinam, 1995; Tsaousi et al., 2010; Vermes et al., 2001).

One of the genotoxicity evidences is formation of micronuclei, which are extranuclear chromosome fragments that forms whenever a chromosome or a fragment of a chromosome is not incorporated into one of the daughter nuclei during cell division. Chromosomal breakage (clastogenic effect) or chromosome separations (aneugenic effect) caused by clastogen or anogen substances in DNA induce micronucleus formation, an evidence for a genotoxic effect (De Souza et al., 2020). In the present study, we conducted a micronucleus test (OECD 487) whether the modified bioglass induces a genotoxic effect on Chinese hamser ovary (CHO) cells either in the presence or absence of S9, a metabolic activator. We concluded that the modified bioglass does not induce genotoxicity as the micronucleus test found no evidence for it.

In this study, we also evaluated the untreated, bioglass kept in SBF, and modified bioglass for their osteoblastic activities and healing morphology in a rat defect model. Especially during the early healing phase (1st and 2nd months) of the defect sites, the defect site treated with the modified bioglass exhibited a significantly higher healing properties compared to all. Thus, the present study has proved a support to previously reported in vitro studies. Various amino acids have been shown to positively affect osteogenic activity and mineralization in vitro (Rautaray et al., 2005; Sarig, 2004; Torricelli et al., 2002). In another study, Chevalley et al. (1998) reported that the addition of arginine to the culture medium increased the synthesis of IGF-1 and collagen in mouse osteoblast cells. The combination of arginine and L-lysine increased osteoblast proliferation and type-1 collagen synthesis in vitro (Trippel, 1998). The results of the present study, the modified glass provided a better healing support especially during the early phase, suggesting that the aminoacid modified bioglass should further be studied for osteoinductivity and osteoconductivity through various molecular technique to unveil the mechanisms behind. In the rat defect model, the defect sites were also evaluated for the local effect following implantation, an in vivo biocompatibility study to determine any irritant effect at defect sites and the surrounding tissues (ISO 10993–6). Similarly, the modified glass did not induce and any irritant with a better scores compared to other treatments; thus, the amino acid modified bioglass is biocompatible with no local irritant effect. Howe.

5 | CONCLUSION

In conclusion, the amino acid modified bioglass has better osteogenic potential and biocompatibility in vitro an in vivo compared to the untreated bioglass and bioglass kept in SBF, especially during the early healing phase of the bone defects. With an improved biocompatibility, better cell attachment property, fostering cell survival, increased ALP activity and calcium accumulation, the amino acid modified bioglass significantly contributes to healing process. Thus, the amino acid modified bioglass is an appropriate material for bone tissue engineering. The future studies should focus mainly on molecular basis of bone healing, osteoinductivity and osteoconductivity properties.

AUTHOR CONTRIBUTIONS

Yasin Özkabadayı: Investigation; writing – original draft; conceptualization; methodology; visualization; project administration; writing – review and editing. **Mustafa Türk:** Conceptualization; methodology; writing – review and editing; supervision. **Ali Kumandaş:** Writing – review and editing; methodology; investigation. **Siyami Karahan:** Conceptualization; investigation; writing – original draft; writing – review and editing; methodology; project administration; validation; supervision.

DATA AVAILABILITY STATEMENT

The data that support the findings of this study are available from the corresponding author upon reasonable request.

ORCID

Yasin Özkabadayı https://orcid.org/0000-0003-0326-3407

REFERENCES

Adawy, A., Abdel-Fattah, W. I., El-Sayed, E. S. M., & Talaat, M. S. (2009). Biomimetic coating of precalcified Ti-6Al-4V alloy. *Open Medical Devices Journal*, *1*, 19–28. https://doi.org/10.2174/1875181400901010019

Agarwal, R., & García, A. J. (2019). Surface modification of biomaterials. In *Principles of regenerative medicine* (pp. 651–660). Academic Press. https://doi.org/10.1016/B978-0-12-809880-6.00037-0

Anderson, J. M. (2001). Biological responses to materials. *Annual Review of Materials Research*, *31*(1), 81–110. https://doi.org/10.1146/annurev.matsci.31.1.81

Anderson, J. M., Rodriguez, A., & Chang, D. T. (2008). Foreign body reaction to biomaterials. In *Seminars in immunology* (Vol. 20, pp. 86–100). Academic Press. https://doi.org/10.1016/j.smim.2007.11.004

Atala, A., Kasper, F. K., & Mikos, A. G. (2012). Engineering complex tissues. *Science Translational Medicine*, *4*(160), 160rv12. https://doi.org/10.1126/scitranslmed.3004890

Baino, F., Hamzehlou, S., & Kargozar, S. (2018). Bioactive glasses: Where are we and where are we going? *Journal of Functional Biomaterials*, *9*(1), 25. https://doi.org/10.3390/jfb9010025

Bayraktar, D., & Tas, A. C. (1999). Chemical preparation of carbonated calcium hydroxyapatite powders at 37 C in urea-containing synthetic body fluids. *Journal of the European Ceramic Society*, *19*(13–14), 2573–2579. https://doi.org/10.1016/S0955-2219(99)00132-6

Beck, G. R., Jr. (2003). Inorganic phosphate as a signaling molecule in osteoblast differentiation. *Journal of Cellular Biochemistry*, *90*(2), 234–243. https://doi.org/10.1002/jcb.10622

Beresford, J. N., Graves, S. E., & Smoothy, C. A. (1993). Formation of mineralized nodules by bone derived cells in vitro: A model of bone formation? *American Journal of Medical Genetics*, *45*(2), 163–178. https://doi.org/10.1002/ajmg.1320450205

Beutler, E. (1989). Nutritional and metabolic aspects of glutathione. *Annual Review of Nutrition*, *9*(1), 287–302. https://doi.org/10.1146/annurev.nu.09.070189.001443

Boanini, E., Torricelli, P., Gazzano, M., Giardino, R., & Bigi, A. (2006). Nanocomposites of hydroxyapatite with aspartic acid and glutamic acid and their interaction with osteoblast-like cells. *Biomaterials*, *27*(25), 4428–4433. https://doi.org/10.1016/j.biomaterials.2006.04.019

Cao, W., & Hench, L. L. (1996). Bioactive materials. *Ceramics International*, *22*(6), 493–507. https://doi.org/10.1016/0272-8842(95)00126-3

Chevalley, T. H., Rizzoli, R., Manen, D., Caverzasio, J., & Bonjour, J. P. (1998). Arginine increases insulin-like growth factor-I production and collagen synthesis in osteoblast-like cells. *Bone*, *23*(2), 103–109. https://doi.org/10.1016/S8756-3282(98)00081-7

Clupper, D. C., Gough, J. E., Hall, M. M., Clare, A. G., LaCourse, W. C., & Hench, L. L. (2003). In vitro bioactivity of S520 glass fibers and initial assessment of osteoblast attachment. *Journal of Biomedical Materials Research Part A*, *67*(1), 285–294. https://doi.org/10.1002/jbm.a.10040

Comesaña, R., Lusquiños, F., Del Val, J., López-Álvarez, M., Quintero, F., Riveiro, A., … Pou, J. (2011). Three-dimensional bioactive glass implants fabricated by rapid prototyping based on CO2 laser cladding. *Acta Biomaterialia*, *7*(9), 3476–3487. https://doi.org/10.1016/j.actbio.2011.05.023

De Souza, L. P., Lopes, J. H., Ferreira, F. V., Martin, R. A., Bertran, C. A., & Camilli, J. A. (2020). Evaluation of effectiveness of 45S5 bioglass doped with niobium for repairing critical-sized bone defect in in vitro and in vivo models. *Journal of Biomedical Materials Research Part A*, *108*(3), 446–457. https://doi.org/10.1002/jbm.a.36826

Elmore, S. (2007). Apoptosis: A review of programmed cell death. *Toxicologic Pathology*, *35*(4), 495–516. https://doi.org/10.1080/01926230701320337

Emery, S. E., Brazinski, M. S., Koka, A., Bensusan, J. S., & Stevenson, S. (1994). The biological and biomechanical effects of irradiation on anterior spinal bone grafts in a canine model. *JBJS*, *76*(4), 540–548. https://doi.org/10.2106/00004623-199404000-00008

Fini, M., Torricelli, P., Giavaresi, G., Carpi, A., Nicolini, A., & Giardino, R. (2001). Effect of L-lysine and L-arginine on primary osteoblast cultures from normal and osteopenic rats. *Biomedicine & Pharmacotherapy*, *55*(4), 213–220. https://doi.org/10.1016/S0753-3322(01)00054-3

Gough, J. E., Notingher, I., & Hench, L. L. (2004). Osteoblast attachment and mineralized nodule formation on rough and smooth 45S5 bioactive glass monoliths. *Journal of Biomedical Materials Research Part A*, *68*(4), 640–650. https://doi.org/10.1002/jbm.a.20075

Hench, L. L., Splinter, R. J., Allen, W. C., & Greenlee, T. K. (1971). Bonding mechanisms at the interface of ceramic prosthetic materials. *Journal of Biomedical Materials Research*, *5*(6), 117–141. https://doi.org/10.1002/jbm.820050611

Hunter, N. L., & Sherman, R. E. (2017). Combination products: Modernizing the regulatory paradigm. *Nature Reviews Drug Discovery*, *16*(8), 513–514. https://doi.org/10.1038/nrd.2017.66

ISO 10993-6 (2016). Biological evaluation of medical devices — Part 6: Tests for local effects after implantation. ISO: Geneva, Switzerland, 2016. Available online: https://www.iso.org/cms/render/live/en/sites/isoorg/contents/data/standard/06/10/61089.html (accessed on 20 June 2021).

Kasuga, T., Hosoi, Y., Nogami, M., & Niinomi, M. (2001). Apatite formation on calcium phosphate invert glasses in simulated body fluid. *Journal of the American Ceramic Society*, *84*(2), 450–452. https://doi.org/10.1111/j.1151-2916.2001.tb00676.x

Keating, J. F., Simpson, A. H. R. W., & Robinson, C. M. (2005). The management of fractures with bone loss. *The Journal of Bone & Joint Surgery British*, *87*(2), 142–150. https://doi.org/10.1302/0301-620X.87B2.15874

Kerr, J. F., Wyllie, A. H., & Currie, A. R. (1972). Apoptosis: A basic biological phenomenon with wide-ranging implications in tissue kinetics. *British Journal of Cancer*, *26*(4), 239–257. https://doi.org/10.1038/bjc.1972.33

Keselowsky, B. G., Collard, D. M., & García, A. J. (2003). Surface chemistry modulates fibronectin conformation and directs integrin binding and specificity to control cell adhesion. *Journal of Biomedical Materials Research Part A*, *66*(2), 247–259. https://doi.org/10.1002/jbm.a.10537

Kim, E. J. B. S. Y., Sung, M. K., & Choi, M. K. (2013). Effects of silicon on osteoblast activity and bone mineralization of MC3T3-E1 cells. *Biological Trace Element Research*, *152*, 105–112. https://doi.org/10.1007/s12011-012-9593-4

Kim, S. R., Lee, J. H., Kim, Y. T., Riu, D. H., Jung, S. J., Lee, Y. J., … Kim, Y. H. (2003). Synthesis of Si, Mg substituted hydroxyapatites and their sintering behaviors. *Biomaterials*, *24*(8), 1389–1398. https://doi.org/10.1016/S0142-9612(02)00523-9

Kokubo, T., & Takadama, H. (2006). How useful is SBF in predicting in vivo bone bioactivity? *Biomaterials*, *27*(15), 2907-2915. https://doi.org/10.1016/j.biomaterials.2006.01.017

Kundu, B., Lemos, A., Soundrapandian, C., Sen, P. S., Datta, S., Ferreira, J. M. F., & Basu, D. (2010). Development of porous HAp and β-TCP scaffolds by starch consolidation with foaming method and drug-chitosan bilayered scaffold based drug delivery system. *Journal of Materials Science: Materials in Medicine*, *21*, 2955–2969. https://doi.org/10.1007/s10856-010-4127-0

Lee, W. H., Loo, C. Y., Van, K. L., Zavgorodniy, A. V., & Rohanizadeh, R. (2012). Modulating protein adsorption onto hydroxyapatite particles using different amino acid treatments. *Journal of the Royal Society Interface*, *9*(70), 918–927. https://doi.org/10.1098/rsif.2011.0586

Lee, W. H., Loo, C. Y., Zavgorodniy, A. V., & Rohanizadeh, R. (2013). High protein adsorptive capacity of amino acid-functionalized hydroxyapatite. *Journal of Biomedical Materials Research Part A*, *101*(3), 873–883. https://doi.org/10.1002/jbm.a.34383

Lopez, J., & Tait, S. W. G. (2015). Mitochondrial apoptosis: Killing cancer using the enemy within. *British Journal of Cancer*, *112*(6), 957–962. https://doi.org/10.1038/bjc.2015.85

Marsell, R., & Einhorn, T. A. (2011). The biology of fracture healing. *Injury*, *42*(6), 551–555. https://doi.org/10.1016/j.injury.2011.03

McConkey, D. J. (1998). Biochemical determinants of apoptosis and necrosis. *Toxicology Letters*, *99*(3), 157–168. https://doi.org/10.1016/S0378-4274(98)00155-6

Mitra, J., Tripathi, G., Sharma, A., & Basu, B. (2013). Scaffolds for bone tissue engineering: Role of surface patterning on osteoblast response. *RSC Advances*, *3*(28), 11073–11094. https://doi.org/10.1039/C3RA23315D

Mohanan, P. V., & Rathinam, K. (1995). Biocompatibility studies on silicone rubber. Proceedings of the first regional conference, IEEE engineering in medicine and biology society and 14th conference of the Biomedical Engineering Society of India. An International Meet. 4–11. https://doi.org/10.1109/RCEMBS.1995.533005

Mollazadeh, S., Javadpour, J., & Khavandi, A. (2007). In situ synthesis and characterization of nano-size hydroxyapatite in poly (vinyl alcohol) matrix. *Ceramics International*, *33*(8), 1579–1583. https://doi.org/10.1016/j.ceramint.2006.06.006

Ohtsuki, C., Kokubo, T., & Yamamuro, T. (1992). Mechanism of apatite formation on CaOSiO2P2O5 glasses in a simulated body fluid. *Journal of Non-Crystalline Solids*, *143*, 84–92. https://doi.org/10.1016/S0022-3093(05)80556-3

Quarto, N., Senarath-Yapa, K., Renda, A., & Longaker, M. T. (2015). TWIST1 silencing enhances in vitro and in vivo osteogenic differentiation of human adipose-derived stem cells by triggering activation of BMP-ERK/FGF signaling and TAZ upregulation. *Stem Cells*, *33*(3), 833–847. https://doi.org/10.1002/stem.1907

Rahmany, M. B., & Van Dyke, M. (2013). Biomimetic approaches to modulate cellular adhesion in biomaterials: A review. *Acta Biomaterialia*, *9*(3), 5431–5437. https://doi.org/10.1016/j.actbio.2012.11.019

Raisz, L. G. (1999). Physiology and pathophysiology of bone remodeling. *Clinical Chemistry*, *45*(8), 1353–1358. https://doi.org/10.1093/clinchem/45.8.1353

Ramaswamy, Y., Wu, C., Zhou, H., & Zreiqat, H. (2008). Biological response of human bone cells to zinc-modified Ca–Si-based ceramics. *Acta*

Biomaterialia, *4*(5), 1487–1497. https://doi.org/10.1016/j.actbio.2008.04.014

Rautaray, D., Mandal, S., & Sastry, M. (2005). Synthesis of hydroxyapatite crystals using amino acid-capped gold nanoparticles as a scaffold. *Langmuir*, *21*(11), 5185–5191. https://doi.org/10.1021/la048541f

Ravarian, R., Moztarzadeh, F., Hashjin, M. S., Rabiee, S. M., Khoshakhlagh, P., & Tahriri, M. (2010). Synthesis, characterization and bioactivity investigation of bioglass/hydroxyapatite composite. *Ceramics International*, *36*(1), 291–297. https://doi.org/10.1016/j.ceramint.2009.09.016

Saboori, A., Rabiee, M., Moztarzadeh, F., Sheikhi, M., Tahriri, M., & Karimi, M. (2009). Synthesis, characterization and in vitro bioactivity of sol-gel-derived SiO2–CaO–P2O5–MgO bioglass. *Materials Science and Engineering: C*, *29*(1), 335–340. https://doi.org/10.1016/j.msec.2008.07.004

Sarig, S. (2004). Aspartic acid nucleates the apatite crystallites of bone: A hypothesis. *Bone*, *35*(1), 108–113. https://doi.org/10.1016/j.bone.2004.02.020

Silva, S. S., Ferreira, R. A., Fu, L., Carlos, L. D., Mano, J. F., Reis, R. L., & Rocha, J. (2005). Functional nanostructured chitosan–siloxane hybrids. *Journal of Materials Chemistry*, *15*(35–36), 3952–3961. https://doi.org/10.1039/b505875a

Silver, I. A., Deas, J., & Erecińska, M. (2001). Interactions of bioactive glasses with osteoblasts in vitro: Effects of 45S5 bioglass®, and 58S and 77S bioactive glasses on metabolism, intracellular ion concentrations and cell viability. *Biomaterials*, *22*(2), 175–185. https://doi.org/10.1016/S0142-9612(00)00173-3

Tas, A. C. (2000). Combustion synthesis of calcium phosphate bioceramic powders. *Journal of the European Ceramic Society*, *20*, 2389–2394.

Torricelli, P., Fini, M., Giavaresi, G., & Giardino, R. (2001). Bone tissue cultures: An in vitro model for the evaluation of bone defect healing after L-arginine and L-lysine administration. *Artificial Cells, Blood Substitutes, and Biotechnology*, *29*(4), 325–334. https://doi.org/10.1081/BIO-100104234

Torricelli, P., Fini, M., Giavaresi, G., Giardino, R., Gnudi, S., Nicolini, A., & Carpi, A. (2002). L-arginine and L-lysine stimulation on cultured human osteoblasts. *Biomedicine & Pharmacotherapy*, *56*(10), 492–497. https://doi.org/10.1016/S0753-3322(02)00287-1

Trippel, S. B. (1998). Potential role of insulinlike growth factors in fracture healing. *Clinical Orthopaedics and Related Research*, *1976-2007*(355), S301–S313. https://doi.org/10.1097/00003086-199810001-00031

Tsaousi, A., Jones, E., & Case, C. P. (2010). The in vitro genotoxicity of orthopaedic ceramic (Al2O3) and metal (CoCr alloy) particles. *Mutation Research/Genetic Toxicology and Environmental Mutagenesis*, *697*(1–2), 1–9. https://doi.org/10.1016/j.mrgentox.2010.01.012

Uddin, M. H., Matsumoto, T., Ishihara, S., Nakahira, A., Okazaki, M., & Sohmura, T. (2010). Apatite containing aspartic acid for selective protein loading. *Journal of Dental Research*, *89*(5), 488–492. https://doi.org/10.1177/0022034509357309

Valerio, P., Pereira, M. M., Goes, A. M., & Leite, M. F. (2004). The effect of ionic products from bioactive glass dissolution on osteoblast proliferation and collagen production. *Biomaterials*, *25*(15), 2941–2948. https://doi.org/10.1016/j.biomaterials.2003.09.086

Variola, F., Vetrone, F., Richert, L., Jedrzejowski, P., Yi, J. H., Zalzal, S., Clair, S., Sarkissian, A., Perepichka, D., Wuest, J. D., Rosei, F., & Nanci, A. (2009). Improving biocompatibility of implantable metals by nanoscale modification of surfaces: An overview of strategies, fabrication methods, and challenges. *Small*, *5*(9), 996–1006. https://doi.org/10.1002/smll.200801186

Ventre, M., Causa, F., & Netti, P. A. (2012). Determinants of cell–material crosstalk at the interface: Towards engineering of cell instructive materials. *Journal of the Royal Society Interface*, *9*(74), 2017–2032. https://doi.org/10.1098/rsif.2012.0308

Vermes, C., Chandrasekaran, R., Jacobs, J. J., Galante, J. O., Roebuck, K. A., & Glant, T. T. (2001). The effects of particulate wear debris, cytokines, and growth factors on the functions of MG-63 osteoblasts. *JBJS*, *83*(2), 201. https://doi.org/10.2106/00004623-200102000-00007

Zhang, Y., Huang, X., Duan, B., Wu, L., Li, S., & Yuan, X. (2007). Preparation of electrospun chitosan/poly (vinyl alcohol) membranes. *Colloid and Polymer Science*, *285*, 855–863. https://doi.org/10.1007/s00396-006-1630-4

How to cite this article: Özkabadayı, Y., Türk, M., Kumandaş, A., & Karahan, S. (2025). Amino acid surface modified bioglass: A candidate biomaterial for bone tissue engineering. *Microscopy Research and Technique*, *88*(1), 26–41. https://doi.org/10.1002/jemt.24659